ISSN 2307-8960 (online)

World Journal of *Clinical Cases*

World J Clin Cases 2021 October 6; 9(28): 8280-8626

Published by Baishideng Publishing Group Inc

World Journal of Clinical Cases

Contents Thrice Monthly Volume 9 Number 28 October 6, 2021

REVIEW

MINIREVIEWS

ORIGINAL ARTICLE

Case Control Study

Retrospective Study

World Journal of Clinical Cases

Thrice Monthly Volume 9 Number 28 October 6, 2021

Contents

World Journal of Clinical Cases

Thrice Monthly Volume 9 Number 28 October 6, 2021

Contents

World Journal of Clinical Cases

Thrice Monthly Volume 9 Number 28 October 6, 2021

Contents

ABOUT COVER

Editorial Board Member of *World Journal of Clinical Cases*, Domenico De Berardis, MD, PhD, Adjunct Professor, Chief Doctor, NHS, Department of Mental Health, Teramo 64100, Italy. domenico.deberardis@aslteramo.it

AIMS AND SCOPE

The primary aim of *World Journal of Clinical Cases* (*WJCC*, *World J Clin Cases*) is to provide scholars and readers from various fields of clinical medicine with a platform to publish high-quality clinical research articles and communicate their research findings online.

WJCC mainly publishes articles reporting research results and findings obtained in the field of clinical medicine and covering a wide range of topics, including case control studies, retrospective cohort studies, retrospective studies, clinical trials studies, observational studies, prospective studies, randomized controlled trials, randomized clinical trials, systematic reviews, meta-analysis, and case reports.

INDEXING/ABSTRACTING

The *WJCC* is now indexed in Science Citation Index Expanded (also known as SciSearch®), Journal Citation Reports/Science Edition, Scopus, PubMed, and PubMed Central. The 2021 Edition of Journal Citation Reports® cites the 2020 impact factor (IF) for *WJCC* as 1.337; IF without journal self cites: 1.301; 5-year IF: 1.742; Journal Citation Indicator: 0.33; Ranking: 119 among 169 journals in medicine, general and internal; and Quartile category: Q3. The *WJCC*'s CiteScore for 2020 is 0.8 and Scopus CiteScore rank 2020: General Medicine is 493/793.

RESPONSIBLE EDITORS FOR THIS ISSUE

Production Editor: *Yan-Xia Xing*; **Production Department Director:** *Yu-Jie Ma*; **Editorial Office Director:** *Jin-Lei Wang*.

NAME OF JOURNAL
World Journal of Clinical Cases

ISSN
ISSN 2307-8960 (online)

LAUNCH DATE
April 16, 2013

FREQUENCY
Thrice Monthly

EDITORS-IN-CHIEF
Dennis A Bloomfield, Sandro Vento, Bao-Gan Peng

EDITORIAL BOARD MEMBERS
https://www.wjgnet.com/2307-8960/editorialboard.htm

PUBLICATION DATE
October 6, 2021

INSTRUCTIONS TO AUTHORS
https://www.wjgnet.com/bpg/gerinfo/204

GUIDELINES FOR ETHICS DOCUMENTS
https://www.wjgnet.com/bpg/GerInfo/287

GUIDELINES FOR NON-NATIVE SPEAKERS OF ENGLISH
https://www.wjgnet.com/bpg/gerinfo/240

PUBLICATION ETHICS
https://www.wjgnet.com/bpg/GerInfo/288

PUBLICATION MISCONDUCT
https://www.wjgnet.com/bpg/gerinfo/208

ARTICLE PROCESSING CHARGE
https://www.wjgnet.com/bpg/gerinfo/242

STEPS FOR SUBMITTING MANUSCRIPTS
https://www.wjgnet.com/bpg/GerInfo/239

ONLINE SUBMISSION
https://www.f6publishing.com

World Journal of Clinical Cases

Submit a Manuscript: https://www.f6publishing.com

World J Clin Cases 2021 October 6; 9(28): 8482-8491

DOI: 10.12998/wjcc.v9.i28.8482

ISSN 2307-8960 (online)

CASE REPORT

Postmenopausal women with hyperandrogenemia: Three case reports

Xiao-Dan Zhu, Lin-Yu Zhou, Jian Jiang, Tian-An Jiang

ORCID number: Xiao-Dan Zhu 0000-0001-8815-3797; Lin-Yu Zhou 0000-0002-8598-1885; Jian Jiang 0000-0003-3618-5943; Tian-An Jiang 0000-0002-7672-8394.

Author contributions: Zhu XD drafted the manuscript, collected the data, and reviewed the literature; Zhou LY and Jiang J performed the histological examination and reviewed the manuscript; Jiang TA provided academic help, and critically reviewed the manuscript; All authors have confirmed and approved the final manuscript.

Supported by National Natural Science Foundation of China, No. 81971623, and No. 82027803.

Informed consent statement: Informed written consent was obtained from patients for publication of this report and any accompanying images.

Conflict-of-interest statement: The authors declare that they have no conflict of interest.

CARE Checklist (2016) statement: The authors have read the CARE Checklist(2016), and the manuscript was prepared and revised according to the CARE Checklist (2016).

Open-Access: This article is an

Xiao-Dan Zhu, Lin-Yu Zhou, Jian Jiang, Tian-An Jiang, Department of Ultrasound Medicine, The First Affiliated Hospital of Zhejiang University School of Medicine, Hangzhou 310006, Zhejiang Province, China

Corresponding author: Tian-An Jiang, MD, Chief Physician, Director, Department of Ultrasound Medicine, The First Affiliated Hospital of Zhejiang University School of Medicine, No. 79 Qingchun Road, Hangzhou 310006, Zhejiang Province, China. tiananjiang@zju.edu.cn

Abstract

BACKGROUND

Diagnosing hyperandrogenemia in postmenopausal women is very difficult. It occasionally manifests as excessive hair growth or with no clinical manifestations, and is therefore often misdiagnosed or missed altogether. Ovarian steroid cell tumors that cause hyperandrogenemia in women account for approximately 0.1% of all ovarian tumors. Due to the low incidence, corresponding imaging reports are rare, so ovarian steroid cell tumors lacks typical imaging findings to differentiate it from other ovarian tumors. Therefore, we summarized its clinical and imaging characteristics through this case series, and elaborated on the differential diagnosis of steroid cell tumors.

CASE SUMMARY

We report three cases of postmenopausal women with hyperandrogenemia. Only 1 patient showed virilization symptoms, the other two patients were completely asymptomatic. All patients underwent total hysterectomy + bilateral adnexectomy. Histological results showed one case of Leydig cell tumor and two cases of benign, non-specific steroid cell tumor. After the operation, the androgen levels of all patients returned to normal, and there was no clinical recurrence since follow-up.

CONCLUSION

Although virilization caused by increased serum testosterone levels is an important clinical feature of ovarian steroid cell tumors, it is often asymptomatic. A solid, slightly hypoechoic, round or oval mass with uniform internal echo, richer blood flow in the solid part, and low resistance index are typical imaging features of ovarian steroid cell tumors. Diagnosis of ovarian steroid cell tumors after menopause is challenging, but surgery can be used for both diagnosis and clear treatment.

Manuscript source: Unsolicited manuscript

Specialty type: Radiology, nuclear medicine and medical imaging

Country/Territory of origin: China

Peer-review report's scientific quality classification

Grade A (Excellent): 0
Grade B (Very good): B
Grade C (Good): 0
Grade D (Fair): 0
Grade E (Poor): 0

Received: March 12, 2021
Peer-review started: March 12, 2021
First decision: June 24, 2021
Revised: July 5, 2021
Accepted: August 18, 2021
Article in press: August 18, 2021
Published online: October 6, 2021

P-Reviewer: Mittal M
S-Editor: Gong ZM
L-Editor: Filipodia
P-Editor: Xing YX

Key Words: Ovarian steroid cell tumor; Postmenopausal women; Asymptomatic; Imaging features; Case report

Core Tip: Ovarian steroid cell tumors are a rare sex cord-stromal tumor accounting for approximately 0.1% of all ovarian tumors. Although virilization caused by increased serum testosterone levels is an important clinical feature of ovarian steroid cell tumors, it is often completely asymptomatic. Therefore, while paying attention to the typical imaging features of ovarian steroid cell tumors, we cannot ignore clinically asymptomatic patients, especially postmenopausal women.

Citation: Zhu XD, Zhou LY, Jiang J, Jiang TA. Postmenopausal women with hyperandrogenemia: Three case reports. *World J Clin Cases* 2021; 9(28): 8482-8491
URL: https://www.wjgnet.com/2307-8960/full/v9/i28/8482.htm
DOI: https://dx.doi.org/10.12998/wjcc.v9.i28.8482

INTRODUCTION

Female androgenemia can cause virilization syndromes, such as progressive hirsutism, acne, vocal cord thickening, amenorrhea, breast atrophy, and male pattern baldness. However, the diagnosis of postmenopausal women with hyperandrogenemia is very difficult because the clinical manifestations are commonly absent or comprise mostly hair overgrowth, so the disease is often attributed to normal hormonal changes with ageing. Diseases that cause hyperandrogenemia in women include ovarian functional tumors, polycystic ovary syndrome, congenital adrenal hyperplasia, congenital follicular cell hyperplasia, acanthosis nigricans, and Cushing's syndrome, among others[1]. Ovarian steroid cell tumors (OSCTs) are a rare sex cord-stromal tumor and account for approximately 0.1% of all ovarian tumors[2]. In 2014, the WHO divided them into ovarian steroid cell tumor, not otherwise specified (OSCT-NOS), and ovarian Leydig cell tumors (OLCTs)[3]. OLCTs are very rare, mainly benign, and more common in menopausal women. These tumors usually occur in a unilateral ovary and are small and solid[4]. Most OSCT-NOS lesions consist of a solid, oval mass with a regular shape that occurs in a unilateral ovary, and is mainly benign. The average age of onset is 42 years. Occurrences in postmenopausal women or children are rare[5,6].

CASE PRESENTATION

Chief complaints

Case 1: A 60-year-old female, who had been menopausal for 7 years, presented with a progressive increase in body hair.

Case 2: A 55-year-old female, who had been menopausal for 5 years, presented with a mass in the left appendix on physical examination.

Case 3: A 52-year-old female, who had been menopausal for 1 year, presented with ovarian cysts found on physical examination.

History of present illness

Case 1: The patient with a progressive increase in body hair lasting for 6 mo.

Case 2: The patient's mass had been present for 5 mo, and recently significantly increased in size.

Case 3: The patient's mass had been present for 1 mo.

History of past illness

Case 1: The patient had a history of uterine fibroids and diabetes, and was currently

taking metformin tablets, 0.5 g (Bid), and glimepiride tablets, 2 mg (Qd).

Case 2: The patient was in good health and had no history of special chronic diseases.

Case 3: The patient had a past history of hypertension, adenomyosis with multiple uterine fibroids, and bilateral kidney cysts.

Personal and family history

Cases 1-3: No abnormal personal or family histories.

Physical examination

Case 1: An increased amount of relatively long facial hair, pubic hair, and body hair in the groin area. No skin pigmentation, voice thickening, weight gain, facial fattening, abdominal circumference thickening, or other symptoms were observed.

Cases 2 and 3: There were no obvious abnormalities on physical examination.

Laboratory examinations

Case 1: The serum testosterone hormone level was significantly increased (504.5 ng/dL), but the levels of other sex hormones and tumor markers were normal. A mid-dose dexamethasone suppression test showed that testosterone was not suppressed (before inhibition: androstenedione, 3.7 ng/mL; testosterone, 504.5 ng/dL; and dehydroepiandrosterone sulphate, 65.5 μg/dL; after inhibition: androstenedione, 1.6 ng/mL; testosterone, 244.7 ng/dL; dehydrosulphate epiandrosterone, 42.1 μg/dL; and 17a hydroxyprogesterone, 0.1 nmol/L) (Table 1).

Case 2: The serum testosterone hormone level was significantly increased (258.09 ng/dL), and the levels of other sex hormones and tumor markers were normal (Table 1).

Case 3: The serum testosterone hormone level was significantly increased (326.03 ng/dL), but the levels of other sex hormones and tumor markers were normal (Table 1).

Imaging examinations

Case 1: Transvaginal ultrasonography (TVS) revealed atrophy of the uterus and bilateral ovaries. A slightly hyperechoic nodule with a diameter of approximately 1.23 cm was observed in the right ovary, with an unclear boundary (Figure 1A). Unfortunately, no blood flow images were available. Abdominal ultrasound showed normal liver, gallbladder, spleen and pancreas, and ascites was not detected. Enhanced magnetic resonance imaging (MRI) of the pelvis (Figure 2A) showed nodules in the right adnexal area, suggesting ovarian cysts. Contrast-enhanced computed tomography (CT) of the pelvis (Figure 2B) showed high-density shadows in the nodular tip of the right adnexal area, suggesting a sex cord-stromal tumor (Table 2).

Case 2: TVS revealed atrophy of the uterus. The left ovary showed a slightly hyperechoic mass of approximately 3.0 cm × 2.2 cm × 3.4 cm in size (Figure 1B), with clear borders (Table 2). Color Doppler flow imaging (CDFI) showed an abundant blood supply (Figure 3A), with a resistance index (RI) of 0.39. Abdominal ultrasound showed normal liver, gallbladder, spleen and pancreas, and ascites was not detected. Enhanced MRI of the pelvis revealed a space-occupying mass in the left adnexal area, suggesting a sex cord-stromal tumor (Figure 2C).

Case 3: TVS indicated a trend of uterine atrophy, with cystic and solid changes in the left ovary (Table 2). A solid, slightly hyperechoic mass of approximately 4.3 cm × 2.9 cm × 2.8 cm in size was observed in the left ovary (Figure 1C), with clear boundaries. CDFI showed an abundant blood supply in the mass (Figure 3B), with an RI of 0.55. Abdominal ultrasound showed normal liver, gallbladder, spleen and pancreas, and ascites was not detected. Enhanced CT of the pelvis showed a solid/cystic mass in the left adnexal area, suggesting a left uterine broad ligament fibroid with central degeneration (Figure 2D).

Table 1 Biochemical parameters determined before and after surgery

Test (units/reference range)	Case 1		Case 2		Case 3	
	Before surgery	After surgery	Before surgery	After surgery	Before surgery	After surgery
LH (mUI/mL) (11.3-40.0)	9.91	18.58	16.98	38.61	6.72	ND
FSH (mUI/mL) (9.7-111.0)	22.9	48.7	20.75	107.99	14.88	ND
Total testosterone (ng/dL) (10.83-56.94)	504.5	35.7	258.09	17.5	326.03	21.25
Oestradiol (pg/mL) (< 30)	51	11.8	73.21	10	71.38	ND
Progesterone (ng/mL)	0.49	0.3	0.43	0.1	0.24	ND
Androstenedione (ng/mL) (0.3-3.3)	1.6	ND	2	ND	1.7	ND
DHEA-S (mg/dL)	42.1	ND	50.5	ND	44.3	ND
17 OHP (ng/mL) (0.2–1.7)	1.7	ND	ND	ND	ND	ND
17 OHP (ng/mL) 600 after ACTH stimulation test	0.1	ND	ND	ND	ND	ND

17 OHP: 17 hydroxyprogesterone; ACTH: Adrenocorticotropic hormone; DHEA-S: Dehydroepiandrosterone-sulfate; FSH: Follicle-stimulating hormone; LH: Luteinizing hormone; ND: Not done.

Table 2 Radiological features

	Case 1	Case 2	Case 3
Pelvic ultrasound	Hyperechoic nodule of Ro (12.3 mm)	Hyperechoic mass of Lo (34 mm× 22 mm)	Hyperechoic mass of Lo (45 mm × 20 mm)
Pelvic CT	Nodular slightly dense shadow of Ro with visible enhancement after enhancement	ND	Oval slightly lower density mass of left adnexal area uneven enhancement after enhancement, continuous enhancement in venous phase
Pelvic MRI	Round-shaped abnormal signal range of Ro, T2W1 and DW1 are high signal, higher signal area can be seen in the center	A circular signal shadow of Lo, equal to T1 long and T2 signal, DWI high signal, and obviously enhanced after enhancement	ND

CT: Computed tomography; Lo: Left ovary; MRI: Magnetic resonance imaging; ND: Not done; Ro: Right ovary.

FINAL DIAGNOSIS

Case 1

Pathology indicated an LCT (Figure 4A): calretinin (CR) (+), chromogranin A (CgA) (-), cytokeratin (CK) (pan) (focus +), inhibin A (+), Ki-67 (6%), S-100 (-), CD99 (-), and smooth muscle actin (SMA) (-).

Case 2

Pathology showed an SCT-NOS lesion (Figure 4B): CK7 (-), CK (pan) (-), paired-box gene 8 (PAX-8) (-), inhibin A (+), CR (+), placental alkaline phosphatase (PLAP) (-), Wilms' tumor gene (WT1) (-), Oct-4 (-), glypican 3 (GPC-3) (-), beta human chorionic gonadotropin (β-HCG) (-), Ki-67 (+, 3%), CD99 (+), S-100 (-), CD117 (-), CD30 (weak +), net dye (+), and E-cadherin (-).

Case 3

Pathology indicated an SCT-NOS lesion: CK (pan) (part +), estrogen receptor (ER) (-), progesterone receptor (PR) (-), inhibin A (+), CR (+), WT1 (-), human melanoma black 45 (HMB-45) (-), MelanA (+), CgA (-), synaptophysin (Syn) (-), Desmin (-), Ki-67 (+, 20%), CD34 (-), and epithelial membrane antigen (EMA) (-).

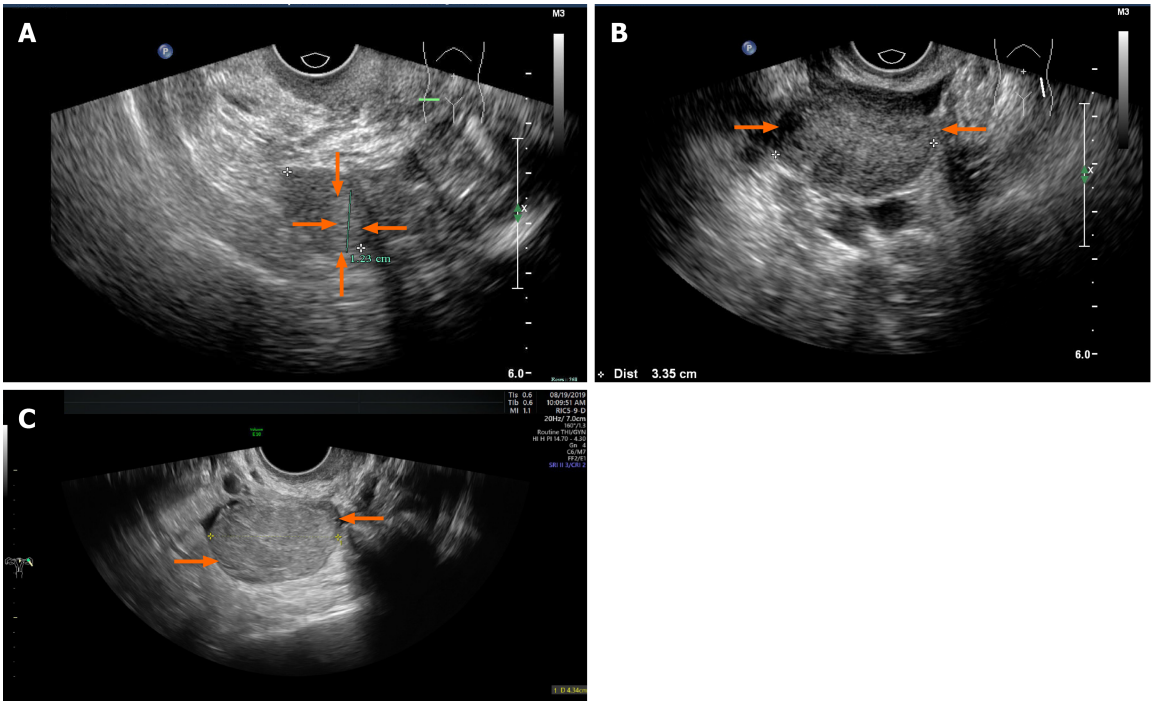

Figure 1 Transvaginal ultrasonography. A: A slightly hyperechoic nodule with an unclear boundary in the right ovary (case 1); B: The left ovary showed a slightly hyperechoic mass with clear boundary (case 2); C: A solid, slightly hyperechoic mass with clear boundary in the left ovary (case 3).

TREATMENT

Case 1

The patient underwent total hysterectomy + bilateral adnexectomy. A grey-white nodule with a diameter of approximately 1.7 cm was observed on the cut surface of the pathological specimen after the operation.

Case 2

The patient underwent total hysterectomy + bilateral adnexectomy. A clear, greyish-yellow, round nodule was observed on pathology after surgery, with a diameter of 2.3 × 3.0 cm.

Case 3

The patient underwent total hysterectomy + bilateral appendectomy. Intraoperative dissection showed that the left ovarian fluid was yellow and turbid, the cyst wall was thickened, and the inner section consisted of tough, yellowish tissue.

OUTCOME AND FOLLOW-UP

Case 1

The testosterone level of the patient was 57.1 ng/dL on the first postoperative day; the virilization symptoms gradually subsided. Follow-up after surgery continued for about 37 mo with no signs of clinical recurrence.

Case 2

The testosterone level of the patient was 17.5 ng/dL after the operation. Follow-up after surgery continued for about 21 mo with no signs of clinical recurrence.

Case 3

The testosterone level of the patient was 21.25 ng/dL after the operation. Follow-up after surgery continued for about 19 mo with no signs of clinical recurrence.

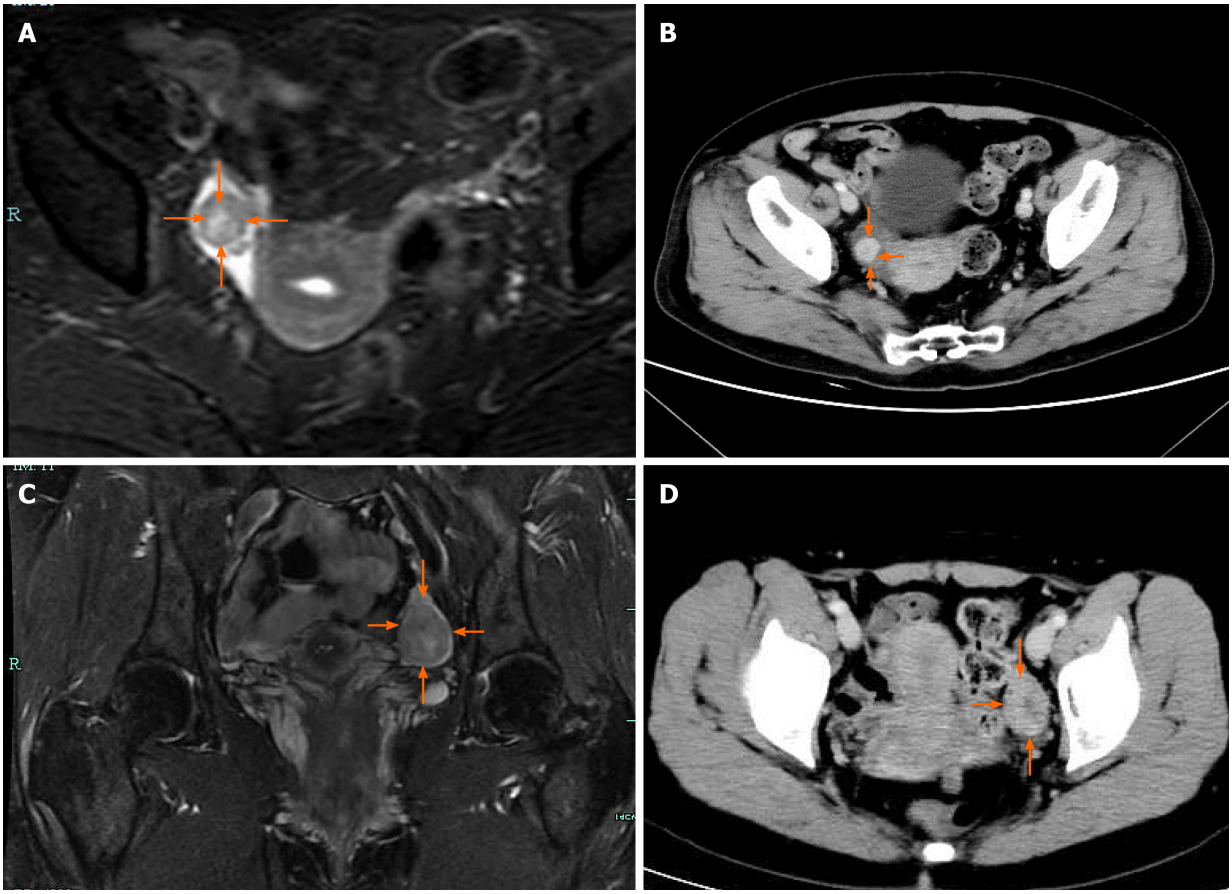

Figure 2 Enhanced magnetic resonance imaging (A and C) and computed tomography (B and D). A: Enhanced magnetic resonance imaging (MRI) of the pelvis showed nodules in the right adnexal area (case 1); B: Contrast computed tomography (CT) of the pelvis showed high-density shadows in the nodular tip of the right adnexal (case 1); C: Enhanced MRI of the pelvis revealed a space-occupying mass in the left adnexal area (case 2); D: Enhanced CT of the pelvis showed a solid/cystic mass in the left adnexal area (case 3).

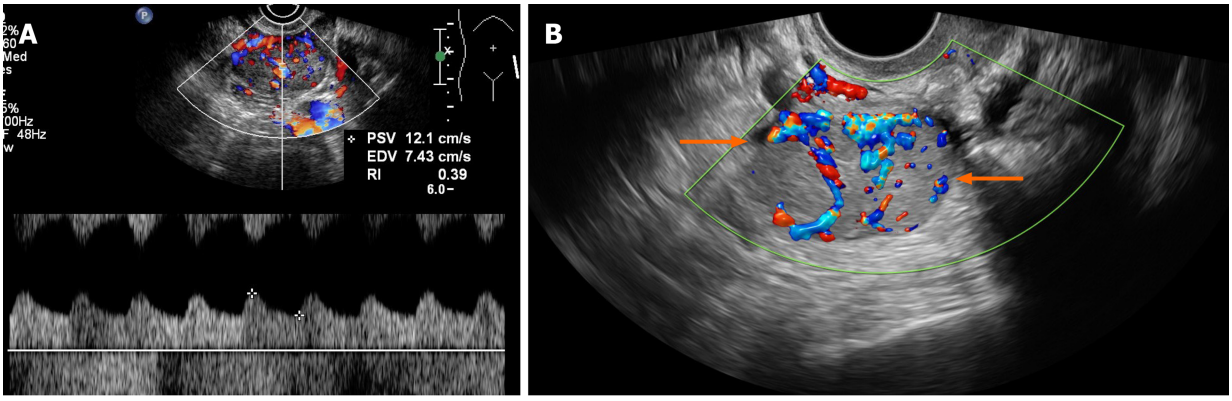

Figure 3 Color Doppler flow imaging. A: Color Doppler flow imaging (CDFI) showed an abundant blood supply with a resistance index of 0.39 (case 2); B: CDFI showed an abundant blood supply in the mass (case 3).

DISCUSSION

Sex cord-stromal tumors are classified into three main groups according to the WHO, and include pure stromal tumors, pure sex cord tumors, and mixed sex cord stromal tumors[7]. OSCTs belongs to a subtype of pure stromal tumors and is an ovarian tumor composed entirely or mostly of cells that secrete steroid hormones. OSCTs can secrete one or more steroid hormones, such as androgens, estrogen, cortisol, aldosterone, and progesterone, resulting in corresponding symptoms and signs, such as hyperandrogenemia, hyperestrogenia, Cushing syndrome, and refractory hypertension, with androgenemia as the most common[8]. In female hyperandro-

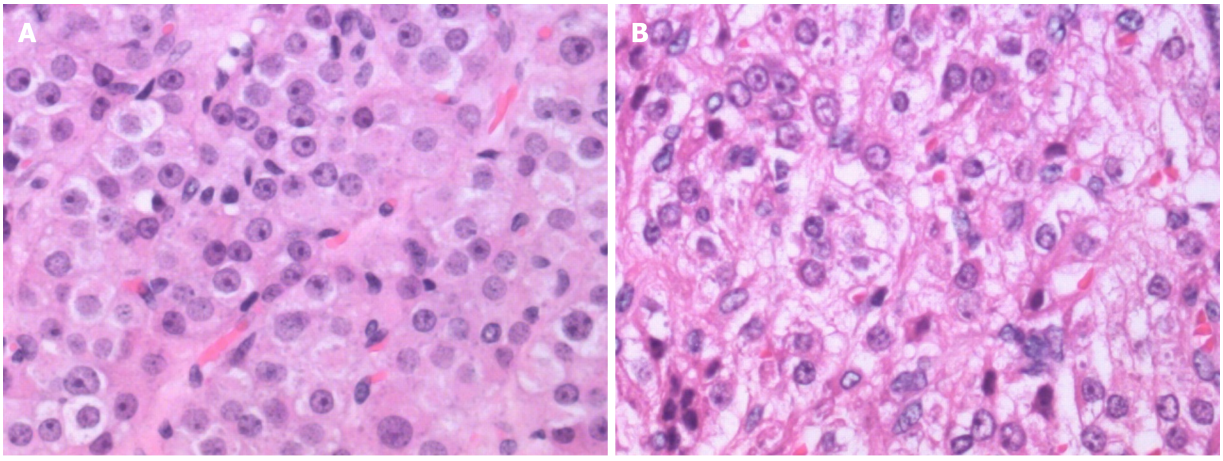

Figure 4 Hematoxylin-eosin staining. A: Hematoxylin-eosin staining by microscopy, × 400 magnification showed Leydig cell tumor (case 1); B: Hematoxylin-eosin staining by microscopy, × 400 magnification showed steroid cell tumor, not otherwise specified (cases 2 and 3).

genism, adrenal and/or ovarian sources need to be distinguished. The cause of hyperandrogenemia caused by adrenal tumors is the secretion of excessive dehydroepiandrosterone sulphate[9], and the androgens secreted by most ovarian tumors are not regulated by gonadotropins or adrenocorticotropic hormone (ACTH). Therefore, adrenal CT and medium-dose dexamethasone suppression tests can be used to exclude adrenal sources. In case 1, the dose of dexamethasone experiment showed that testosterone was not inhibited, which confirmed this view.

The clinical manifestations of OSCTs are determined by the steroid hormones produced, and OSCTs can be divided into high-androgen types and high-estrogen types. Most OSCTs (80%) are of the high-androgen type, and approximately 20% of OSCTs are of the high-estrogen type[10,11]. High-androgen-type tumors mainly cause symptoms such as hirsutism, acne, a low and thick voice, an enlarged clitoris, laryngeal knots, breast atrophy, hair loss, and a low posterior hairline. High-estrogen-type tumors mainly cause symptoms such as irregular vaginal bleeding and endometrial hyperplasia. All patients in this case series exhibited high-androgen-type OSCTs. In case 1, the patient showed progressive hirsutism, and the patients in cases 2 and 3 showed no obvious clinical symptoms. We reviewed and summarized 87 cases of OSCTs reported in the English literature from 2000 to 2019, and found that only one case was reported as having no clinical symptoms[12]. All other OSCT patients will have corresponding clinical symptoms caused by endocrine abnormalities. In addition, clinical symptoms, such as abdominal pain and masses in the lower abdomen, can also occur. However, this asymptomatic patient has a long-term history of taking contraceptives, and OSCT was found during the diagnosis and treatment of infertility; the patient became pregnant naturally after tumor resection. Therefore, whether infertility is caused by OSCT is still inconclusive. In our case series, there are 2 cases without any clinical manifestations, so we believe that being clinically asymptomatic is one of the clinical features of OSCT that should be acknowledged.

Due to the low incidence of OSCTs, corresponding imaging reports are rare, and most of them are case reports, so the typical imaging features are not fully understood. Additionally, due to lack of clinical symptoms, particularly in postmenopausal patients, the patient is more likely to have a missed diagnosis or be misdiagnosed. On histology, OSCTs are generally well-defined and spherical, while LCTs are significantly smaller than SCT-NOS lesions. OSCTs are dominated by solid components; because most of them contain fat components, they were once called lipocytomas. On microscopy, the tumor cells are rich in lipids, and there are abundant capillary networks and vascular sinusoid structures in the tumor[13]. Ultrasound is the first choice for the detection and diagnosis of ovarian tumors due to its convenience, speed and non-invasiveness. OSCTs tend to occur in one ovary, and grey-scale ultrasound usually shows solid, round or oval nodules with clear boundaries. The internal echo is mainly slightly hyperechoic. The echo intensity may be related to the internal fat content. Because testosterone has the effect of increasing vasodilatory substances, most OSCTs exhibit rich blood flow signals dominated by low-resistance blood flow[14]. Since LCTs are very small and lack typical imaging features, this may cause poor visibility on ultrasound and CT examinations[15,16]. At the same time, in menopausal women, due to the reduced estrogen level and insufficient perfusion by

the ovarian artery blood, the appearance of the ovaries is reduced, and the echo of the ovaries is increased. CDFI usually indicates no blood flow signals in the ovaries[17]. Therefore, it is difficult to distinguish between OLCT tissue and normal atrophic ovarian tissue by ultrasound. At present, it is believed that SCT-NOS lesions are more easily recognized on imaging than LCTs.

Mature teratomas contain liquid fat and appear as a clear hyperechoic mass on grey-scale ultrasound. Thus, teratomas need to be differentiated from OSCTs. Especially when a small, hyperechoic mass appears on one ovary in menopausal women, the possibility of an OLCT cannot be ignored. However, most teratomas are mixed tumors with cystic and solid component. Lipid stratification can occur in the cystic part, and some of the lesions can contain bone tissue or teeth, appearing as hyperechoic nodules with rear acoustic shadows. CDFI usually shows no obvious blood flow signal these masses. Because teratomas contain very few non-secretory tissues that produce testosterone, they very rarely cause hyperandrogenism[18].

Thecoma that secrete estrogen are composed of lipid-rich ovarian membrane cells. Histologically, these tumors are mainly solid, with a hard texture and intact capsule, which can be combined with various forms of degeneration, such as calcification. On grey-scale ultrasound, thecoma appear as a round or lobulated, hypoechoic mass with a smooth surface and are often accompanied by varying degrees of posterior sound attenuation, with clear or unclear boundaries; the internal echoes may be uniform or uneven. CDFI shows no obvious blood flow signals in thecoma, and estrogen secretion is the main distinguishing feature of OSCTs[19]. McGonagall syndrome can occur when the tumor is large.

Follicular membrane fibroids are derived from spindle-shaped collagen fibroblasts. They are sex cord-stromal tumors that occur in perimenopausal or postmenopausal women with inactive hormone secretion, and rarely become malignant. It accounts for 4% of all ovarian tumors, and often occurs in unilateral ovary. It is reported that the membrane fibroma may be related to Gorlin syndrome[20]. Follicular membrane fibromas and thecomas have similar features on grey-scale ultrasound. CDFI shows that these mass have no blood supply or secretory function, which are key to distinguishing follicular membrane fibromas from OSCTs.

When broad ligament leiomyomas become large and show degenerative changes, it is difficult to distinguish them from ovarian tumors. Therefore, accurate positioning of the ovary is the key to distinguishing between the two. Whirlpool or woven hypoechoic masses and pseudocapsules are characteristic ultrasound manifestations of leiomyomas. CDFI shows low blood flow signals inside and around these tumors. Similarly, the lack of endocrine function is also key to distinguishing leiomyomas from OSCTs.

Malignant sex cord stromal tumors arise from the primitive sex cord and/or stromal cells of the gonads, including granulosa, theca, Sertoli, or Leydig cells, as well as fibroblasts[21]. One of the most common subtypes is granulosa cell tumor (GCT), the adult and juvenile granulosa cell histological subtypes comprise the majority (> 70%) of malignant sex cord stromal tumors. GCTs are rare, low-grade ovarian stromal tumors with a granular cell morphology, and most secrete estrogen, which can induce endometrial hyperplasia. Endometrial hyperplasia and endometrial cancer, which is associated with GCTs, can manifest as abnormal uterine bleeding[21]. GCT is usually between 5 and 15 cm, and > 95% occurs unilaterally. Because GCT tissue is fragile and easily becomes detached, causing hemorrhagic necrosis and cystic transformation, the cut surfaces are typically solid and cystic with fluid or blood-filled cysts separated by solid, yellow to white, soft to firm tissue. So solid/cystic masses are typical imaging features of ovarian GCTs, and they are mostly arranged in intervals in a radial pattern. CDFI shows minimal to moderate blood flow signals in these tumors[22], with mostly low-resistance blood flow due to the vasodilator effect of estrogen. It is not difficult to distinguish ovarian GCTs from OSCTs using both clinical and imaging features.

Ovarian Sertoli-Leydig cell tumors (OSLCTs) with androgen secreting function is a subtype of malignant sex cord stromal tumor, second only to OGCT. Unlike OSCT patients, approximately 75% of patients with SLCTs are 30-years-old or younger, and only 10% > 50-years-old. They are composed of Sertoli cells and/or mesenchymal cells of different levels. Histologically, OSLCTs mainly manifest as a hard, lobulated mass, yellow to brown solid cross section with a complete capsule[23]. The tumor is usually cystic when it contains heterologous or retiform components. Tumors with a large, heterologous mucinous components may resemble a mucinous cystic tumor. The cysts in the retiform tumors may contain papillary or polypoid excrescences, potentially resembling a serous tumor[24]. On grey-scale ultrasound, OSLCTs are mainly solid/cystic masses with clear boundaries. Because the tumor cells contain more fibrous interstitium, the solid part of the tumor is less echogenic. Most of these tumors

are rich in blood vessels, so they can show an abundant blood supply on imaging.

SCT-NOS lesions are the most prone to malignant transformation among OSCTs, with a malignant transformation rate of approximately 25%-43%[14]. When OSCTs undergo malignant transformation, necrosis, hemorrhage and cystic transformation may occur, and these OSCTs need to be differentiated from ovarian cystadenocarcinomas. Cystadenocarcinomas are malignant ovarian epithelial tumors, with an age at onset later than that of OSCTs. The grey-scale ultrasound features of serous cystic carcinomas include a single sac or cystic mass with compartments, usually accompanied by papillary protrusions. Mucinous cystadenocarcinomas are very large and are usually multilocular cystic masses with solid wall nodules, turbid cyst fluid and poor sound transmission. Since ovarian malignant tumor cells can produce vascular endothelial growth factor, *etc*., they can induce the formation of new blood vessels lacking smooth muscle tissue, which will lead to a low blood flow RI[25]. On CDFI, the solid component of ovarian cystadenocarcinomas shows abundant low-resistance blood flow signals. At the same time, the presence of endocrine function can also help further distinguish the type of tumor. It should be noted that Ki-67 is used as a tumor stem cell marker, and the research scope is mainly ovarian epithelioid tumors. Some studies believe that the Ki-67 index can help evaluate the malignancy and prognosis of ovarian tumors. When the positive cells are less than 10%, there is basically no recurrence. However, some studies have found that the distribution of positive cells in different parts of the same tumor is quite different. Therefore, there is some controversy in the evaluation of ovarian tumors. In Case 3, although Ki-67 (+, 20%), the pathological results still suggest benign SCT-NOS, and there are no signs of recurrence after about 14 mo of follow-up. Therefore, the evaluation and classification of SCT-NOS and outcome prediction still need to be integrated consider.

CONCLUSION

In summary, the diagnosis of postmenopausal OSCTs is mainly based on typical symptoms and signs, sex hormone determination, imaging features and pathological findings. The corresponding symptoms caused by endocrine abnormalities are the most intuitive clinical manifestations of the disease, especially virilization caused by hyperandrogenemia, which is more common, but there are still some patients who are completely asymptomatic. A solid, slightly hypoechoic, round or oval mass with a uniform internal echo and an abundant blood supply with low resistance are more typical imaging features of OSCTs. Diagnosing OSCTs is challenging, and surgery can be used for both diagnosis and clear treatment. Of course, histological examination is the gold standard for the final diagnosis of OSCTs.

REFERENCES

1 **Alpañés M**, González-Casbas JM, Sánchez J, Pián H, Escobar-Morreale HF. Management of postmenopausal virilization. *J Clin Endocrinol Metab* 2012; **97**: 2584-2588 [PMID: 22669303 DOI: 10.1210/jc.2012-1683]

2 **Souto SB**, Baptista PV, Braga DC, Carvalho D. Ovarian Leydig cell tumor in a post-menopausal patient with severe hyperandrogenism. *Arq Bras Endocrinol Metabol* 2014; **58**: 68-75 [PMID: 24728167 DOI: 10.1590/0004-2730000002461]

3 **Wang J**, Wu H, Liang Z. Clinical analysis of 19 cases of ovarian steroid cell tumor. *Zhenduan Bingli Zazhi* 2017; **8**: 561-569 [DOI: 10.3969/j.issn.1007-8096.2017.08.001]

4 **Ferrinho C**, Silva E, Oliveira M, Sequeira Duarte J. Ovarian Leydig cell tumor and postmenopausal hirsutism with signs of virilisation. *BMJ Case Rep* 2021; **14** [PMID: 33731391 DOI: 10.1136/bcr-2020-240937]

5 **Amneus MW**, Natarajan S. Pathologic quiz case: a rare tumor of the ovary. *Arch Pathol Lab Med* 2003; **127**: 890-892 [PMID: 12823052 DOI: 10.5858/2003-127-890-PQCART]

6 **Smith D**, Crotty TB, Murphy JF, Crofton ME, Franks S, McKenna TJ. A steroid cell tumor outside the ovary is a rare cause of virilization. *Fertil Steril* 2006; **85**: 227 [PMID: 16412760 DOI: 10.1016/j.fertnstert.2005.06.055]

7 **Al Harbi R**, McNeish IA, El-Bahrawy M. Ovarian sex cord-stromal tumors: an update on clinical features, molecular changes, and management. *Int J Gynecol Cancer* 2021; **31**: 161-168 [PMID: 33414107 DOI: 10.1136/ijgc-2020-002018]

8 **Varras M**, Vasilakaki T, Skafida E, Akrivis C. Clinical, ultrasonographic, computed tomography and histopathological manifestations of ovarian steroid cell tumour, not otherwise specified: our experience of a rare case with female virilisation and review of the literature. *Gynecol Endocrinol* 2011; **27**: 412-418 [PMID: 20586551 DOI: 10.3109/09513590.2010.495432]

9 **Burger HG**. Androgen production in women. *Fertil Steril* 2002; **77** Suppl 4: S3-S5 [PMID: 12007895 DOI: 10.1016/s0015-0282(02)02985-0]

10 **Vulink AJ**, Vermes I, Kuijper P, ten Cate LN, Schutter EM. Steroid cell tumour not otherwise specified during pregnancy: a case report and diagnostic work-up for virilisation in a pregnant patient. *Eur J Obstet Gynecol Reprod Biol* 2004; **112**: 221-227 [PMID: 14746964 DOI: 10.1016/j.ejogrb.2003.06.001]

11 **Hayes MC**, Scully RE. Ovarian steroid cell tumors (not otherwise specified). A clinicopathological analysis of 63 cases. *Am J Surg Pathol* 1987; **11**: 835-845 [PMID: 2823622 DOI: 10.1097/00000478-198711000-00002]

12 **Alves P**, Sá I, Brito M, Carnide C, Moutinho O. An Early Diagnosis of an Ovarian Steroid Cell Tumor Not Otherwise Specified in a Woman. *Case Rep Obstet Gynecol* 2019; **2019**: 2537480 [PMID: 30792930 DOI: 10.1155/2019/2537480]

13 **Murhekar K**, Louis R, Majhi U. A rare occurrence of a steroid cell tumor of the pelvic mesentery: a case report. *J Med Case Rep* 2011; **5**: 517 [PMID: 22008415 DOI: 10.1186/1752-1947-5-517]

14 **Lee J**, John VS, Liang SX, D'Agostino CA, Menzin AW. Metastatic Malignant Ovarian Steroid Cell Tumor: A Case Report and Review of the Literature. *Case Rep Obstet Gynecol* 2016; **2016**: 6184573 [PMID: 27375912 DOI: 10.1155/2016/6184573]

15 **Shanbhogue AK**, Shanbhogue DK, Prasad SR, Surabhi VR, Fasih N, Menias CO. Clinical syndromes associated with ovarian neoplasms: a comprehensive review. *Radiographics* 2010; **30**: 903-919 [PMID: 20631359 DOI: 10.1148/rg.304095745]

16 **Palha A**, Cortez L, Tavares AP, Agapito A. Leydig cell tumour and mature ovarian teratoma: rare androgen-secreting ovarian tumours in postmenopausal women. *BMJ Case Rep* 2016; **2016** [PMID: 27803082 DOI: 10.1136/bcr-2016-215985]

17 **Demidov VN**, Lipatenkova J, Vikhareva O, Van Holsbeke C, Timmerman D, Valentin L. Imaging of gynecological disease (2): clinical and ultrasound characteristics of Sertoli cell tumors, Sertoli-Leydig cell tumors and Leydig cell tumors. *Ultrasound Obstet Gynecol* 2008; **31**: 85-91 [PMID: 18098335 DOI: 10.1002/uog.5227]

18 **Hoffman JG**, Strickland JL, Yin J. Virilizing ovarian dermoid cyst with leydig cells. *J Pediatr Adolesc Gynecol* 2009; **22**: e39-e40 [PMID: 19539195 DOI: 10.1016/j.jpag.2008.05.012]

19 **Chung BM**, Park SB, Lee JB, Park HJ, Kim YS, Oh YJ. Magnetic resonance imaging features of ovarian fibroma, fibrothecoma, and thecoma. *Abdom Imaging* 2015; **40**: 1263-1272 [PMID: 25273949 DOI: 10.1007/s00261-014-0257-z]

20 **Obeidat RA**, Aleshawi AJ, Obeidat HA, Al Bashir SM. A rare presentation of ovarian fibrothecoma in a middle age female: case report. *Int J Womens Health* 2019; **11**: 149-152 [PMID: 30881143 DOI: 10.2147/IJWH.S191549]

21 **Maoz A**, Matsuo K, Ciccone MA, Matsuzaki S, Klar M, Roman LD, Sood AK, Gershenson DM. Molecular Pathways and Targeted Therapies for Malignant Ovarian Germ Cell Tumors and Sex Cord-Stromal Tumors: A Contemporary Review. *Cancers (Basel)* 2020; **12** [PMID: 32485873 DOI: 10.3390/cancers12061398]

22 **Kilinc YB**, Sari L, Toprak H, Gultekin MA, Karabulut UE, Sahin N. Ovarian Granulosa Cell Tumor: A Clinicoradiologic Series with Literature Review. *Curr Med Imaging* 2021; **17**: 790-797 [PMID: 33371855 DOI: 10.2174/1573405616666201228153755]

23 **Schultz KA**, Harris AK, Schneider DT, Young RH, Brown J, Gershenson DM, Dehner LP, Hill DA, Messinger YH, Frazier AL. Ovarian Sex Cord-Stromal Tumors. *J Oncol Pract* 2016; **12**: 940-946 [PMID: 27858560 DOI: 10.1200/JOP.2016.016261]

24 **Young RH**. Ovarian sex cord-stromal tumours and their mimics. *Pathology* 2018; **50**: 5-15 [PMID: 29132723 DOI: 10.1016/j.pathol.2017.09.007]

25 **Gavalas NG**, Liontos M, Trachana SP, Bagratuni T, Arapinis C, Liacos C, Dimopoulos MA, Bamias A. Angiogenesis-related pathways in the pathogenesis of ovarian cancer. *Int J Mol Sci* 2013; **14**: 15885-15909 [PMID: 23903048 DOI: 10.3390/ijms140815885]

Published by **Baishideng Publishing Group Inc**
7041 Koll Center Parkway, Suite 160, Pleasanton, CA 94566, USA
Telephone: +1-925-3991568
E-mail: bpgoffice@wjgnet.com
Help Desk: https://www.f6publishing.com/helpdesk
https://www.wjgnet.com